ASTRONOMY
AND
ASTROPHYSICS

Letter to the Editor

Solar hydrogen lines in the infrared

M. Carlsson[1] **and R. J. Rutten**[2]

[1] Institute of Theoretical Astrophysics, P.O. Box 1029, Blindern, N-0315 Oslo, Norway
[2] Sterrekundig Instituut, Postbus 80 000, NL-3508 TA Utrecht, The Netherlands

Abstract. We study recently observed H I lines in the infrared solar spectrum, employing detailed NLTE modeling to explain their formation and to evaluate their diagnostic merits. The solar infrared H I lines vary much in character, depending on opacity and wavelength; our computations reproduce the observations closely. The line wings are primarily set by Stark broadening due to metal ions and protons; the line cores are sensitive to NLTE population departure divergence which is driven by Balmer-continuum photoionization. The formation heights of the H I lines range from the deep photosphere for near-infrared line wings to the chromosphere for line cores with $\lambda > 10$ μm; these features provide valuable diagnostics of the thermal structure of the solar atmosphere.

Key words: Sun: atmosphere of – Sun: chromosphere of – Sun: photosphere of – line formation – lines: profile – infrared: stars

1. Introduction

Predictions regarding the nature and observability of Rydberg lines in the solar spectrum have steadily progressed towards lower element number and ionization stage, towards lower principal quantum number n, towards shorter wavelengths, and towards lower height of formation, respectively from spectra as O VI to H I, from $n \approx 100$ to $n \approx 10$, from radio to infrared and from corona to chromosphere (Sunyaev & Vainstein 1968, Dupree 1968, Dravskikh & Dravskikh 1969, Greve 1970, 1974, 1975a, 1975b, 1977, Berger & Simon 1972, Shimabukuro & Wilson 1973, Khersonskii & Varshalovich 1980, Hoang-Binh 1982). In this letter we examine the formation of solar H I Rydberg lines with $n = 4 - 18$ in the solar 2–200 μm spectrum, reproducing recent space observations of disk-center profiles in the near infrared and predicting emission strengths in the far infrared.

Pertinent observations are present in the seminal paper of Brault & Noyes (1983), which not only started the Mg I 12 μm literature (reviewed in Carlsson et al. 1992a) but also provides data on H I 12 μm lines seen near the limb and from an off-limb prominence; the latter have been analyzed by Zirker (1985). In the meantime, the Spacelab-3 ATMOS experiment (Farmer & Norton 1989) has yielded disk-center spectra for

---

Send offprint requests to: M. Carlsson

$\sigma = 600 - 4600$ cm^{-1} ($\lambda = 16.7 - 2.2$ μm) which are nearly free from telluric absorption; we use a digital atlas constructed from them by R.L. Kurucz. In addition, Boreiko & Clark (1986) have published balloon observations of a few H I lines at longer wavelengths.

2. Computations

As in our similar analysis of the Rydberg Mg I lines (Carlsson et al. 1992a), we adopt complete frequency redistribution, radial stratification without inhomogeneities as specified either by the empirical MACKKL model (Maltby et al. 1986, Fig. 1) or by the theoretical radiative-equilibrium T5780 model (Edvardsson et al. 1991, Fig. 1), and we set the microturbulence to 1 km s^{-1} at all heights. We solve the statistical equilibrium and radiative transfer equations for all levels, lines and edges in a 19-level-plus-continuum H I model atom, using the operator perturbation technique of Scharmer & Carlsson (1985) as coded in the program MULTI (Carlsson 1986) with the modifications described by Carlsson et al. (1992a).

Level energies were taken from Bashkin & Stoner (1975) for the lowest nine levels and computed adopting $E_n \propto n^{-2}$ for the other levels. Radiative bound-bound transition probabilities come from Johnson (1972), bound-free gaunt factors from Karzas & Latter (1961) and Menzel & Pekeris (1935), collisional transition probabilities from Vriens & Smeets (1980). Line blanketing was taken into account as described in Carlsson et al. (1992a).

Of special importance is the linear Stark broadening by charged particles. Electron broadening was advocated by Greve (1977); we use the second approximation of Sutton (1978). Hoang-Binh (1982) showed that proton collisions are more important; we include them using the equations of Hoang-Binh et al. (1987), employing Voigt rather than Holtsmark line shapes. We also use these equations to enter Stark broadening by heavier ions, taking atomic weight 25 as representative of Na I, Mg I, Al I, Si I etc. The second panel of Fig. 1 shows that the ion contribution is the most important one throughout the photosphere. Proton broadening dominates in the deepest layers; above the temperature minimum, electron broadening dominates for lower-n levels while proton broadening takes over for $n > 5$.
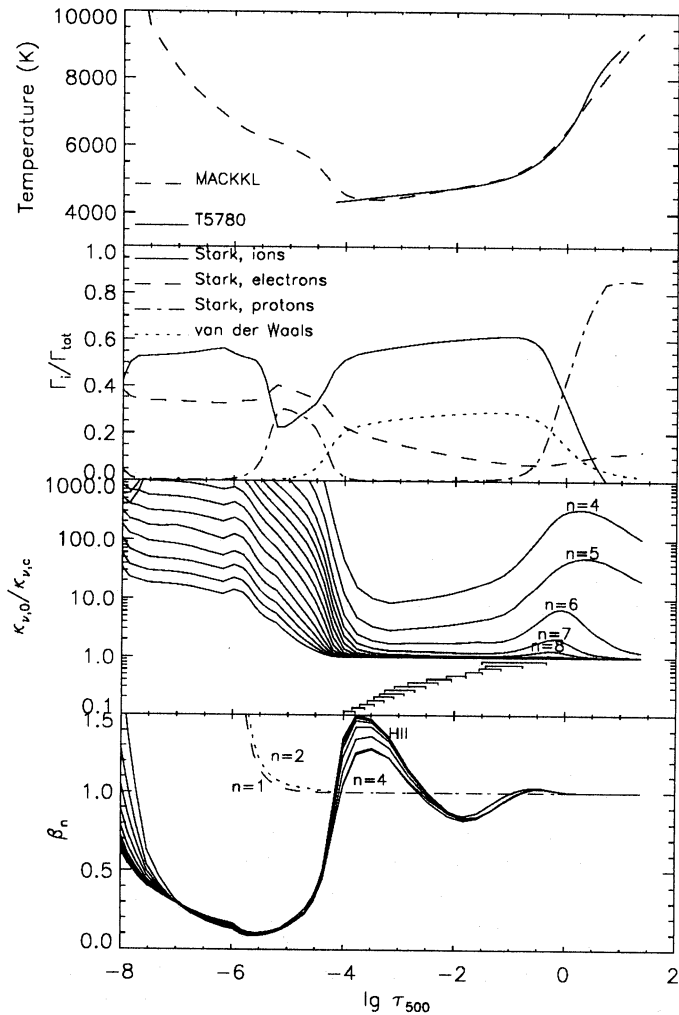
Fig. 1. Various H I line formation quantities against logarithm of continuum optical depth at $\lambda = 500$ nm. Top: temperature stratification of atmospheric models MACKKL (dashed) and T5780 (solid). Note the absence of a chromosphere in T5780. Second panel: relative contributions to broadening of the 5α line, respectively by metal ions, electrons, protons and hydrogen atoms (MACKKL). Note the importance of metal ion broadening in the temperature minimum region. The contribution pattern is similar for other H I Rydberg lines. Third panel: line-to-continuum opacity ratio for $n\alpha$ lines indicated by lower-level quantum number n (MACKKL). Tick marks indicate optical depth unity for the line center and the continuum for $n\alpha$ lines, $n=4$–18 (top to bottom). Bottom: NLTE departure coefficients for the indicated hydrogen levels (MACKKL)

3. Results

Figure 2 shows ATMOS observations overlaid with computed profiles (dashed, MACKKL; solid: T5780). Intensities are plotted in the form of brightness temperature to avoid contrast variations set by the temperature response of the Planck function at different wavelengths.

The general agreement is good. From top to bottom, the lines turn from absorption lines with very wide wings into narrower emission peaks or vanish altogether. This disappearance is not due to diminishing line strength, but to a decrease of the line-to-continuum opacity ratio $\eta_n = \kappa_{\mathrm{line}}/\kappa_{\mathrm{cont}}$; it largely

sets the pattern in Fig. 2. The line opacity κ_{line} at a given height increases from right to left in Fig. 2 ($n\alpha$ lines having larger transition probability than corresponding $n\beta$ lines, etc.) but also from top to bottom because the increase in statistical weight ($g_n \propto n^2$) offsets the decrease of $\exp(-h\nu/kT)$ for $n > 5$. However, the H^- free-free continuum opacity increases steeply with wavelength ($\kappa_{\mathrm{cont}} \propto \lambda^2$), producing rapid decrease of η_n with n (third panel of Fig. 1). In addition, the higher formation height at longer wavelengths samples smaller η_n-values as well, as is shown by the tick marks in the third panel of Fig. 1. These mark the optical depth unity locations for the line center and continuum at each $n\alpha$ line ($n=4$–18 from top to bottom).

The broad wings of the Brackett lines, especially 4β and 4γ, originate quite deep and are only reproduced correctly if Stark broadening by ions is accounted for. Note that we have applied no parameter adjustments; nor is microturbulent broadening important since it is far outweighed by thermal broadening for hydrogen.

The 5α and 6α lines are blended; the upward peak in the latter profile seems due to H I, not the deeper dip at left. There is no ATMOS observation of 7α (lower left), but it is the strongest limb-emission line in Table 2 of Brault & Noyes (1983), while T.A. Clark (private communication) has observed it to reach $I_0/I_{\mathrm{cont}} \approx 1.06$ at disk center, between our two model estimates (Fig. 3).

The slight emission features of the $n\alpha$ lines for the chromosphere-less T5780 model are due to NLTE effects. These act in the H I Rydberg regime much the same way as they do for Mg I Rydberg lines; we therefore describe them briefly with reference to the more detailed discussions in Carlsson et al. (1992a, 1992b) and Bruls et al. (1992). The major differences between H I and Mg I are, first, that H I Rydberg levels have lower populations than Mg I Rydberg levels in the photosphere but higher ones in the chromosphere (Fig. 15 of Carlsson et al. 1992a), and second, that Mg I is a minority species while H I is the majority ionization stage at the heights where infrared Rydberg lines are formed. In both cases, the Rydberg populations are coupled closely between adjacent levels and to the ion population, while a collisional departure diffusion flow passes through the Rydberg levels if there is NLTE population departure difference between the continuum and levels located lower in the term diagram. In that case, the NLTE departures of the Rydberg levels diverge to provide a ladder of $\Delta n = 1$ steps along which collisional net rates maintain the net population flow required to bridge the difference.

In Mg I the continuum has LTE population while the lower boundary condition is set by underpopulation due to photon losses; the resulting population divergence causes the photospheric emission of the Mg I 12 μm lines. In H I, the conditions reverse: the lower boundary condition is set by the LTE populations of the $n = 1$ and $n = 2$ levels, while the continuum is slightly overpopulated in the temperature minimum due to overionization in the Balmer continuum, and strongly underpopulated in the low chromosphere where the electron temperature exceeds the Balmer-continuum radiation temperature. This is shown in the bottom panel of Fig. 1 where H I NLTE population departure coefficients β_n are plotted following Wijbenga & Zwaan (1972). There is slight departure divergence between the levels 4–10 which produces intensity enhancement of lines formed near the temperature minimum.
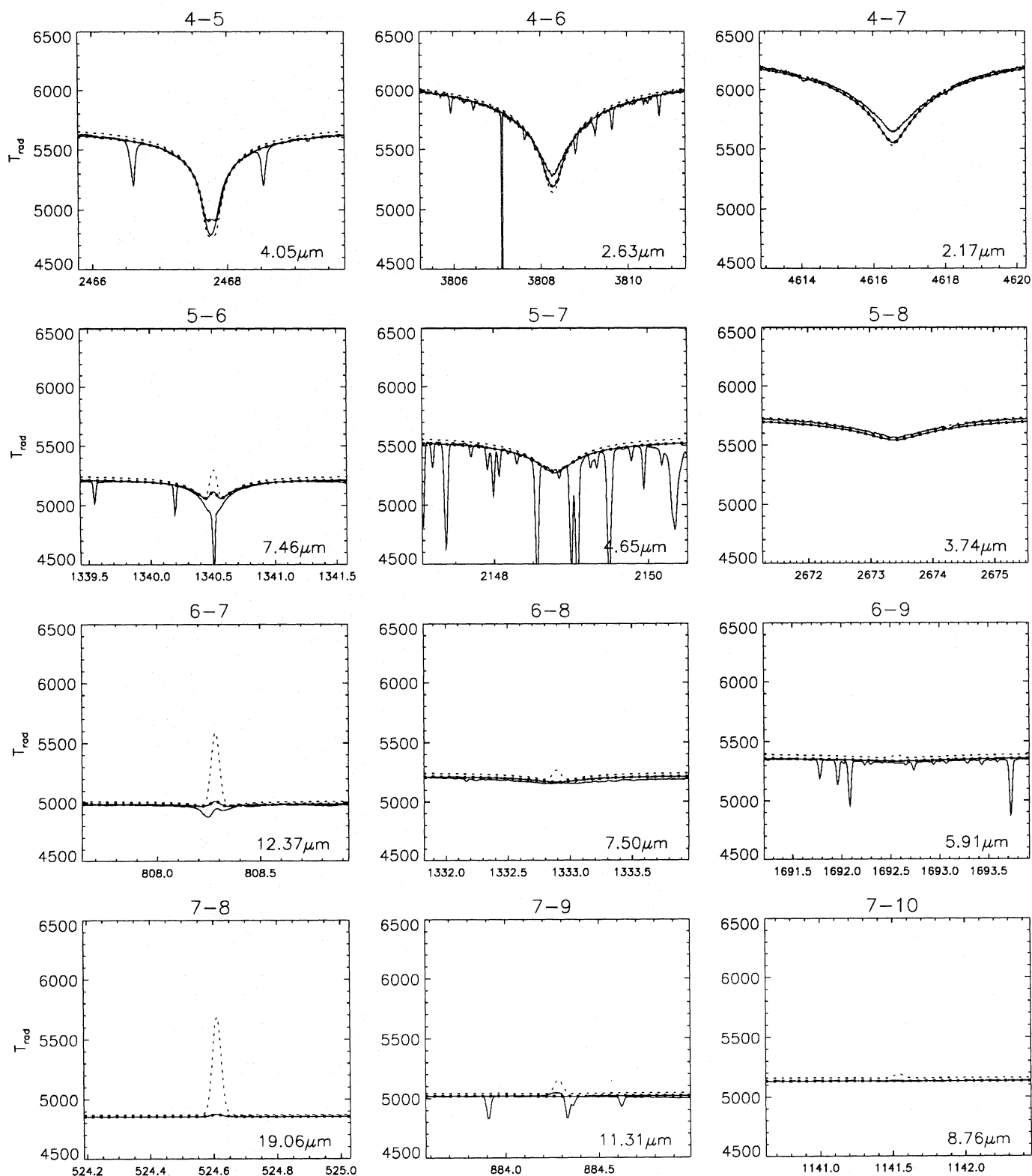
Fig. 2. Comparison of observed H I line profiles from ATMOS (solid) with profiles computed for the MACKKL model (dashed) and the T5780 model (solid+dashed). The ATMOS relative intensities have been converted to absolute intensities using the computed T5780 continuum intensity. Abscissae: wavenumbers in cm^{-1}; corresponding wavelengths are given in each panel. Ordinates: intensity in the form of radiation brightness temperature. There is no ATMOS observation of the 7α (7–8) line

Fig. 3 shows line-center intensities for $n\alpha$ lines up to $n = 18$, normalized by the local continuum intensity. A similar prediction was made earlier by Hoang-Binh (1982), on the basis of chromospheric optically-thin slab modeling. The top curve is for the MACKKL model, the bottom curve for the T5780 model; they bracket the actual emission strengths of the lines observed by Boreiko & Clark (1986) which are shown as (isolated) crosses. The middle curve is for the MACKKL model using the Planck function as line source function; the LTE-to-NLTE differences are largest for the lines with lower level $n = 6 - 9$.
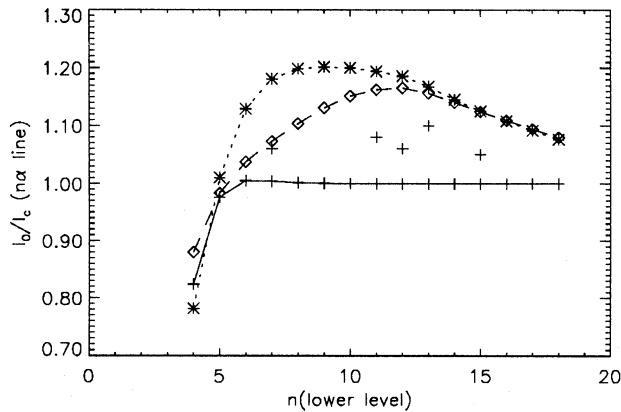

Fig. 3. Predicted emission peak strengths I_0/I_{cont} for far-infrared H I $n\alpha$ lines. Ordinate: lower-level quantum number n. Upper values (dotted curve, asterisks): MACKKL model, NLTE. Middle values (dashed curve, diamonds): MACKKL model, LTE source functions. Lower values (solid curve, crosses): T5780 model, NLTE. The five isolated crosses mark observed peak intensities from Boreiko & Clark

4. Discussion

The computed profiles in Fig. 2 do not fit the observations exactly, but closely enough to give confidence that H I Rydberg line formation in the solar spectrum is basically understood (cf. Zirker 1985). We haven't applied any parameter adjustment; refinements may perhaps be made in atomic physics parameters, primarily Stark broadening formalisms and collision cross-sections.

We have shown results for both MACKKL and T5780, feeling that together these models exhibit the range present in the actual solar chromosphere which is presumably bifurcated into hot magnetic and cooler non-magnetic components. The observations are indeed mostly bracketed by the two computations. The largest differences occur for the cores of the highest-formed lines (6–7 and 7–8), demonstrating sensitivity to the thermal structure of the low chromosphere. The large width of the lines makes them poor measurers of velocities or magnetic fields, nor are their Zeeman splitting patterns clearcut (Greve 1975b). We conclude that their response to upper-atmosphere structuring is the most useful property for future studies employing H I Rydberg lines as solar diagnostics. Fig. 3 shows that NLTE modeling is then required up to $n \approx 15$.

Finally, detailed reproduction of solar H I Rydberg lines as achieved here provides insights in line formation and Stark broadening theory profitable to future stellar studies (cf. Waters & Marlborough 1992).

References

Bashkin, S., Stoner, J. O. 1975, Atomic Energy Levels and Grotrian Diagrams, North-Holland Publ. Co., Amsterdam
Berger, P. S., Simon, M. 1972, ApJ, 171, 191
Boreiko, R. T., Clark, T. A. 1986, A&A, 157, 353
Brault, J., Noyes, R. 1983, ApJ, 269, L61
Bruls, J. H. M. J., Rutten, R. J., Shchukina, N. G. 1992, A&A, submitted
Carlsson, M. 1986, A Computer Program for Solving Multi-Level Non-LTE Radiative Transfer Problems in Moving or Static Atmospheres, Report No. 33, Uppsala Astronomical Observatory
Carlsson, M., Rutten, R. J., Shchukina, N. G. 1992a, A&A, 253, 567
Carlsson, M., Rutten, R. J., Shchukina, N. G. 1992b, in M. Giampapa, J. M. Bookbinder (eds.), Cool Stars, Stellar Systems and the Sun, Proc. Seventh Cambridge Workshop, Astron. Soc. Pac. Conf. Series, in press
Dravskikh, A. F., Dravskikh, Z. V. 1969, SvA, 13, 360
Dupree, A. K. 1968, ApJ, 152, L125
Edvardsson, B., Gustafsson, B., Lambert, D. L., Nissen, P. E., Tomkin, J., Andersen, J. 1991, in preparation
Farmer, C. B., Norton, R. H. 1989, A High-Resolution Atlas of the Infrared Spectrum of the Sun and the Earth Atmosphere from Space, NASA Ref. Publ. 1224, Vol. 1
Greve, A. 1970, Solar Phys., 15, 380
Greve, A. 1974, Solar Phys., 36, 85
Greve, A. 1975a, Solar Phys., 40, 329
Greve, A. 1975b, Solar Phys., 44, 371
Greve, A. 1977, Solar Phys., 52, 423
Hoang-Binh, D. 1982, A&A, 112, L3
Hoang-Binh, D., Brault, P., Picart, J., Tran-Minh, N., Vallée, O. 1987, A&A, 181, 134
Johnson, L. C. 1972, ApJ, 174, 227
Karzas, W. J., Latter, R. 1961, ApJS, 6, 167
Khersonskii, V. K., Varshalovich, D. A. 1980, SvA, 24, 359
Maltby, P., Avrett, E. H., Carlsson, M., Kjeldseth-Moe, O., Kurucz, R. L., Loeser, R. 1986, ApJ, 306, 284
Menzel, D., Pekeris, C. 1935, MNRAS, 96, 77
Scharmer, G. B., Carlsson, M. 1985, J. Comput. Phys., 59, 56
Shimabukuro, F. I., Wilson, W. J. 1973, ApJ, 183, 1025
Sunyaev, R. A., Vainstein, L. A. 1968, Astrophys. Lett., 1, 193
Sutton, K. 1978, J. Quant. Spectrosc. Radiat. Transfer, 20, 333
Vriens, L., Smeets, A. H. M. 1980, Phys. Rev. A, 22, 940
Waters, L. B. F. M., Marlborough, J. M. 1992, A&A, 1992, L25
Wijbenga, J. W., Zwaan, C. 1972, Solar Phys., 23, 265
Zirker, J. B. 1985, Solar Phys., 102, 33